Structural Chemistry
https://doi.org/10.1007/s11224-024-02292-7

RESEARCH

Theoretical analysis of mechanism and regio- and stereoselectivity of 1, 3-dipolar cycloaddition of cyclic nitrone and substituted alkenes by DFT method

Samir Bouacha[1]

Received: 25 August 2023 / Accepted: 4 February 2024

Abstract
This study presents a theoretical investigation of the [3 + 2] cycloaddition (32CA) reaction between cyclic nitrone **a1** and substituted alkene **b1**. The mechanism, regioselectivity, and stereoselectivity of this 32CA reaction were analyzed using transition state theory and reactivity indices obtained from conceptual density functional theory (DFT) at the B3LYP/6-311G(d) level of theory. The results indicate that this cycloaddition reaction proceeds via an asynchronous one-step mechanism, exhibiting a non-polar nature and significant activation energies. These theoretical results are in agreement with the experimental observations. The study also employs topological analyses such as ESP, RDG-NCI, and ELF to determine active sites; distinguish hydrogen bonds, van der Waals interactions, and steric repulsive interactions; and predict electron localization, respectively.

Keywords Cycloaddition · Regioselectivity · Reactivity indices · DFT calculations · Isoxazolidine · Topological analysis

Introduction

The [3 + 2] cycloaddition (32CA) reaction has been extensively employed in synthesizing five-membered heterocyclic compounds [1]. Nitrones, a highly reactive group of reagents, readily partake in 32CA with various dipolarophiles, particularly alkenes, leading to the formation of significant isoxazolidines in excellent yields (Scheme 1) [2]. These cycloadducts have drawn significant attention owing to their potential biological effects. They can serve as precursors of β-amino alcohols through reductive cleavage of the N–O bond. Furthermore, they hold promise as crucial building blocks for synthesizing numerous natural products, including β-lactam antibiotics, alkaloids, as well as sugar and nucleoside analogs [3, 4]. Isoxazolidines possess medicinal properties such as anticonvulsant, antibacterial, antitubercular, antibiotic, and antifungal activities [4].

Several recent studies have focused on the synthesis of isoxazolidine, notably the research carried out by Volkan and colleagues [5]. They produced isoxazolidine derivatives by (32CA) reactions involving α-aryl-N-methyl nitrones and diethyl maleate. The results reveal that all the compounds synthesized show significant activity against *S. epidermidis*, *M. luteus*, *B. cereus*, *B. abortus*, and *C. albicans* compared with standard drugs. Similarly, Bhaskar and Esmita's study [6] focuses on the creation of novel scaffolds of isoxazolidine derivatives using nitrone derived from dihydrofuran by (32CA) reactions under solvent-free conditions, with satisfactory results in both yield and selectivity.

There are many theoretical studies related to the 32CA reactions. Nacereddine and colleagues [7] conducted a theoretical study utilizing FMO analysis to determine the regioselectivity of reactions involving a nitrone derivative and substituted alkenes. The FMO analysis revealed that the substituted alkenes can display both electrophilic and nucleophilic behavior, depending on their specific nature. In another study, Mousa Soleymani and co-authors [8] conducted a theoretical study of (32CA) reaction of 5,5-dimethyl-1-pyrroline N-oxide and 2-cyclopentenone using the molecular electron density theory (MEDT), potential energy surface analysis, transition state theory, and the reactivity indices for the explained reactivity, regioselectivity, and stereospecific and electron density fluxes of the reaction. Furthermore, Ewa et al. [9] executed a theoretical investigation of the (32CA) reaction involving

✉ Samir Bouacha
samir.bouacha@univ-msila.dz

[1] Department of Technology, University of Mohammed Boudiaf, MB 166, M'sila, Algeria

Published online: 14 February 2024

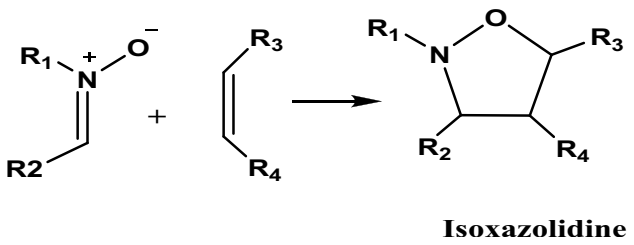

Scheme 1 Synthesis of isoxazolidines by 32CA reaction of nitrones with alkenes substituted

2-methyl-1-nitroprop-1-ene and (Z)-C-aryl-N-phenylnitrones using the B3LYP/6-31G(d) level of theory and MEDT approach to study regioselectivity, stereoselectivity, and molecular mechanisms. The (32CA) processes in this reaction were identified as polar processes with asynchronous transition states. In addition, other reactivity descriptors such as Fukui indices, local softness, and local philicity have been utilized to predict regioselectivity and elucidate variations in reactivity for particular reactions [10, 11].

The primary objective of our research was to explore the theoretical approaches related to the 32CA reaction. Specifically, our focus was on investigating the reaction between cyclic nitrone **a1** and substituted alkene **b1**, which leads to the formation of isoxazolidine, as depicted in Scheme 2 [12]. The aim of our study is to obtain a better understanding of the factors influencing the regio- and stereoselectivity in the 32CA reaction, while also examining the specific molecular mechanism involved in this process.

To achieve this, we utilized FMO analysis, transition state theory, and reactivity indices obtained from conceptual density functional theory. On the other hand, we used the topological analyses such as ESP (electrostatic potential), RDG-NCI (reduced density gradient–non-covalent interactions), and ELF (electron localization function) to identify active sites, distinguish between different types of interactions and steric repulsions, and make predictions about the localization of electrons in the reacting system.

Computational details

In this research, the GAUSSIAN09 software [13] was utilized for all computations. Geometric optimization of reactants, products, and transition states employed density functional theory (DFT) methods at the B3LYP/6-311G(d,p) level [14]. Frequency calculations were performed to characterize the stationary points and verify that the transition states possessed a single imaginary frequency, as expected. To confirm the connectivity between each saddle point and the two associated minima, intrinsic reaction coordinate (IRC) calculations were conducted in both the forward and backward directions [15]. These IRC calculations utilized the second-order González-Schlegel integration method [16, 17]. For further analysis of the electronic structures of the stationary points, natural population analysis (NPA) was employed [18]. This comprehensive approach allowed us to obtain valuable insights about the details of the reaction pathways and the electronic properties of the involved species.

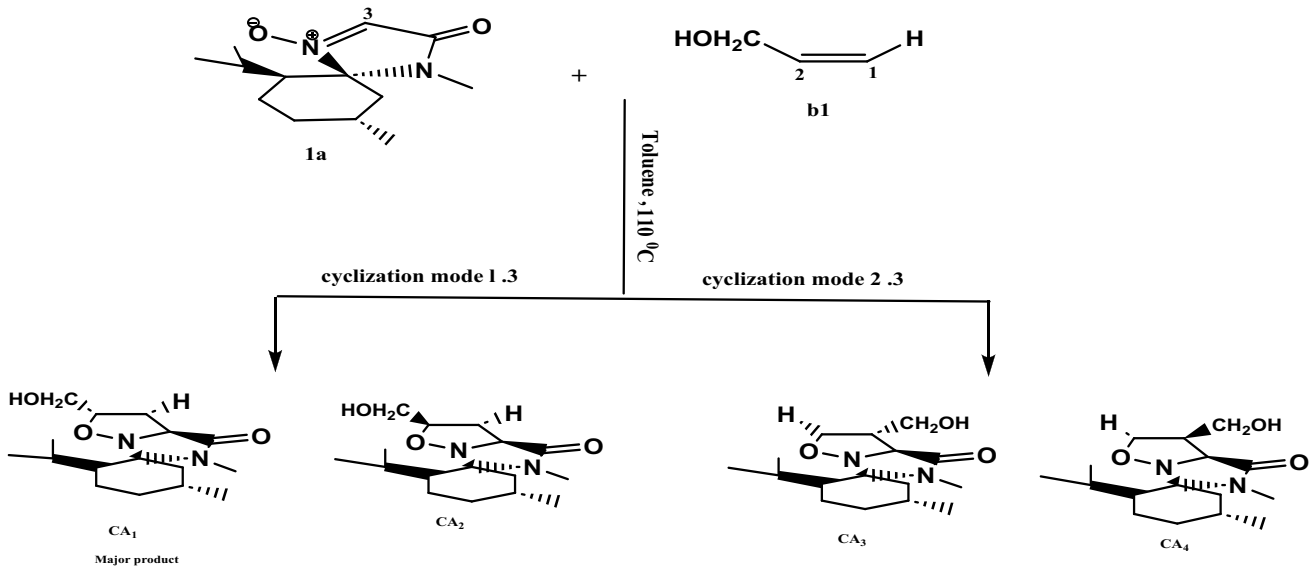

Scheme 2 Experimental results of the [3 + 2] cycloaddition reaction between cyclic nitrone (a1) and alkene (b1) for synthesis of enantiopure isoxazolidines

The influence of toluene as a solvent was taken into account by fully optimizing the gas-phase structures at computational level B3LYP/6-311G(d,P), using the polarizable continuum model (PCM) developed by Tomasi and Persico's group [19]. Gibbs enthalpies, entropies, and free energies in toluene were determined via standard statistical thermodynamics at 110 °C and 1 atm [20].

The global electrophilicity index (ω) is determined using the equation: $\omega = (\mu^2/2\eta)$ [21]. To calculate ω, we need to approximate the chemical hardness (η) and the electronic chemical potential (μ) in terms of the one-electron energies of the highest occupied molecular orbital (HOMO) and lowest unoccupied molecular orbital (LUMO), denoted as ε_H and ε_L, respectively. The chemical hardness (η) can be estimated as $\eta \approx \varepsilon_L - \varepsilon_H$, representing the energy difference between the LUMO and HOMO orbitals, which gives us a measure of the system's resistance to electron exchange or polarization [21]. Similarly, the electronic chemical potential (μ) can be approximated as $\mu \approx (\varepsilon_H + \varepsilon_L)/2$, which represents the average energy of the HOMO and LUMO orbitals and provides insights into the system's ability to donate or accept electrons [22]. The relative nucleophilicity index (N) is determined based on the energies of HOMO within the Kohn–Sham scheme [22]. It can be defined as: $N = \varepsilon_H(\mathrm{Nu}) - \varepsilon_H(\mathrm{TCE})$, where TCE (tetracyanoethylene) is chosen as the reference due to its lowest HOMO energy [21].

Recent research shows the importance of predicting regioselectivity in cycloaddition reactions by focusing on the most favorable reactive pathway. This pathway implies the initial two-center interaction between the most electrophilic and nucleophilic centers of the reactants. Domingo and P'erez [23] recently introduced the electrophilic P_k^+ and nucleophilic P_k^- Parr functions [23], which are derived from changes in spin electron density during the GEDT process from nucleophile to electrophile. These functions serve as potent tools for investigating local reactivity. The electrophilic P_k^+ and nucleophilic P_k^- Parr functions were obtained through the analysis of the Mulliken atomic spin densities (ASD) of the corresponding radical anion and radical cation by single-point energy calculations over the optimized neutral geometries.

The most effective approach to elucidate the reaction mechanism, particularly during electrophilic and nucleophilic attacks, is through the study of electronic surface behavior. A key aspect of this investigation involves the identification and confirmation of the transition state formed. In this study, TS_1 was characterized using various methods, including ESP or MEP (molecular electrostatic potential), reduced density gradient/non-covalent interaction (RDG/NCI), and electron localization function (ELF). To conduct these topological calculations, the researchers utilized MultiWfn software [24] in combination with the VMD program [25].

Results and discussion

In our research, our main objective is to offer a theoretical basis for the observed regioselectivity and stereoselectivity of the nitrone **(a1)** and alkene **(b1)** reaction depicted in Scheme 2. To accomplish this goal, we utilize various theoretical approaches, which include determining activation energies, employing the frontier molecular orbital (FMO) theory, and the electrophilic P_k^+ and nucleophilic P_k^- Parr functions derived from the changes of spin electron-density. It's essential to note that the reaction under study is kinetically controlled, meaning that the final results of the reaction are governed by the relative activation energies.

Prediction and rationalization of experimental regioselectivity

To predict and rationalize the experimentally observed regioselectivity of the 32CA reaction between nitrone **a1** and alkene **b1**, we used two theoretical approaches:

(a) Activation energy calculations

The interaction between nitrone **1a** and alkene **b1** at the 32CA reaction can occur through two regioisomeric channels and two stereoisomeric approaches (see Scheme 2). Consequently, four cycloadducts and the corresponding four transition states have been identified and characterized. Table 1 summarizes the relative energies, relative enthalpies, entropies, and Gibbs free energies of the transition states and the cycloadducts of this reaction.

To study the 32CA reaction, we utilize density functional theory (DFT). Our study includes a computational analysis of the regioselectivity and stereoselec-

Table 1 B3LYP/6-311G (d,p) energies (E, in a.u.), relative energies (ΔE, in kcal /mol), relative enthalpies (ΔH, in kcal/mol), entropies (ΔS, in kcal/mol), and Gibbs free energies (ΔG, in kcal/mol), for the stationary points involved in the 32CA reaction between nitrone 1a and alkene b1 in solvent (toluene)

	E(u.a)	ΔE	ΔH	ΔS	ΔG
a1	− 768.742370	− −			
b1	− 193.172761	− −			
TS_1	− 961.879365	**22.44**	**25.13**	45.75	**42.66**
TS_2	− 961.876851	24.02	26.80	49.42	45.74
TS_3	− 961.875272	25.02	27.89	49.95	47.07
TS_4	− 961.871042	27.66	30.76	51.73	50.59
CA_1	− 961.941294	**− 16.41**	− 11.04	**− 52.27**	**08.98**
CA_2	− 961.933182	− 11.33	− 06.18	− 50.95	12.93
CA_3	− 961.939969	− 15.58	− 11.15	− 56.90	10.64
CA_4	− 961.938786	− 14.84	− 09.22	− 54.53	11.67

tivity in the cycloaddition of nitrone 1a with alkene b1. Our primary objective is to calculate the energy barrier for this reaction. In these computations, the B3LYP/6-311G (d,p) method is utilized with toluene as the solvent. Figure 1 displays the transition states corresponding to the two cyclization modes, 1.3 and 2.3. From Table 1, the activation energy of TS_1 (22.44 kcal/mol) is lower than that of TS_3 (25.02 kcal/mol). Similarly, the activation energy for TS_2 (24.02 kcal/mol) is lower than the TS_4 (27.66 kcal/mol) (see Scheme 3). These results demonstrate that the cyclization mode 1.3 is more kinetically favored than the cyclization mode 2.3. On the other hand, the CA_1 is the most favorable kinetically compared with all other products. These values reflect high regioselectivity and stereoselectivity. Therefore, the present 32CA reaction favors the formation of a single stereoisomer produced from approach 1.3 (CA_1), in agreement with experimental data. Based on the information provided in Table 1, we observe that in this reaction, the cycloadduct CA_1 (-16.41 kcal/mol) is thermodynamically more stabilized compared to the cycloadducts CA_2 (− 11.33 kcal/mol), CA_3 (− 15.58 kcal/mol), and CA_4 (− 14.84 kcal/mol), respectively.

The values of the relative enthalpies, entropies, and Gibbs free energies of the TSs and cycloadducts involved in the reaction of nitrone a1 with alkene b1 are collected in Table 1.

According to Table 1, a comparison of the relative activation enthalpies for the four reactive pathways in the 32CA reaction between nitrone **a1** and alkene **b1** reveals that the most favorable approach mode is consistently associated with TS_1 ($\Delta H = 25.13$ kcal mol^{-1}). The addition of the entropic contribution to the enthalpy increases the activation Gibbs free

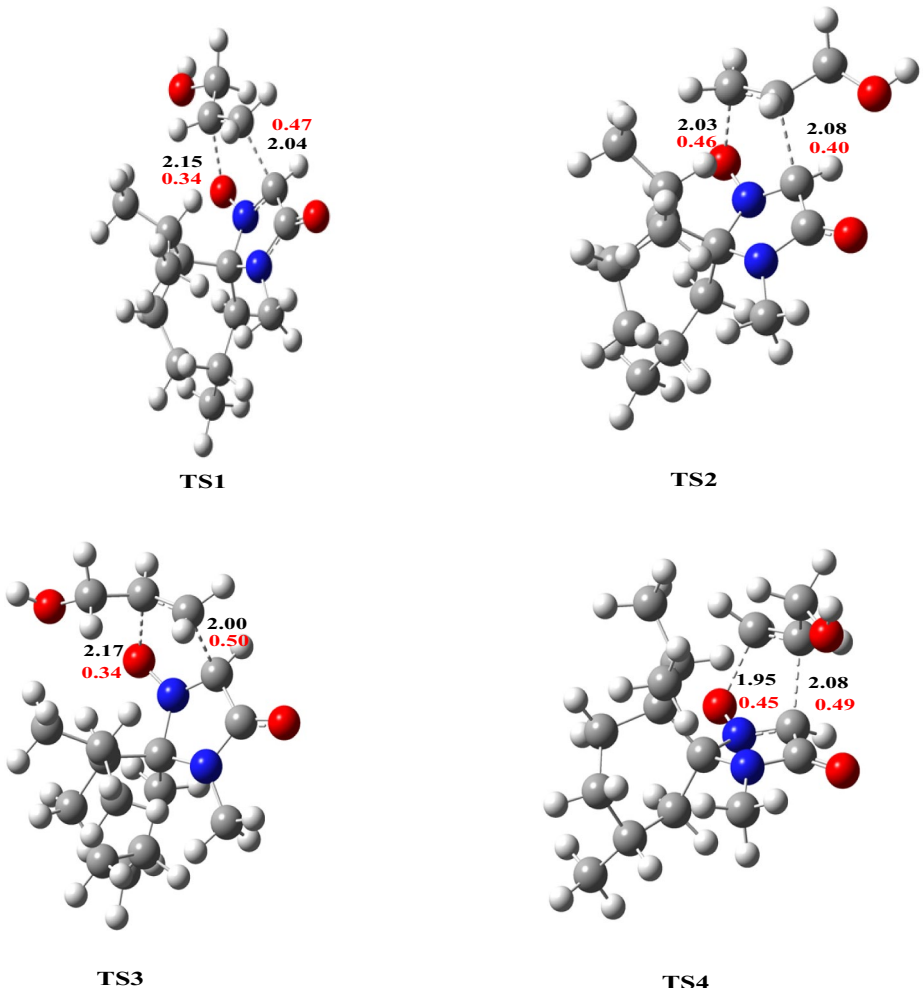

Fig. 1 Transition state structures of 32CA reaction between nitrone a1 and alkene b1 at B3LYP/6-31G* in solvent (toluene), bond order values in red color

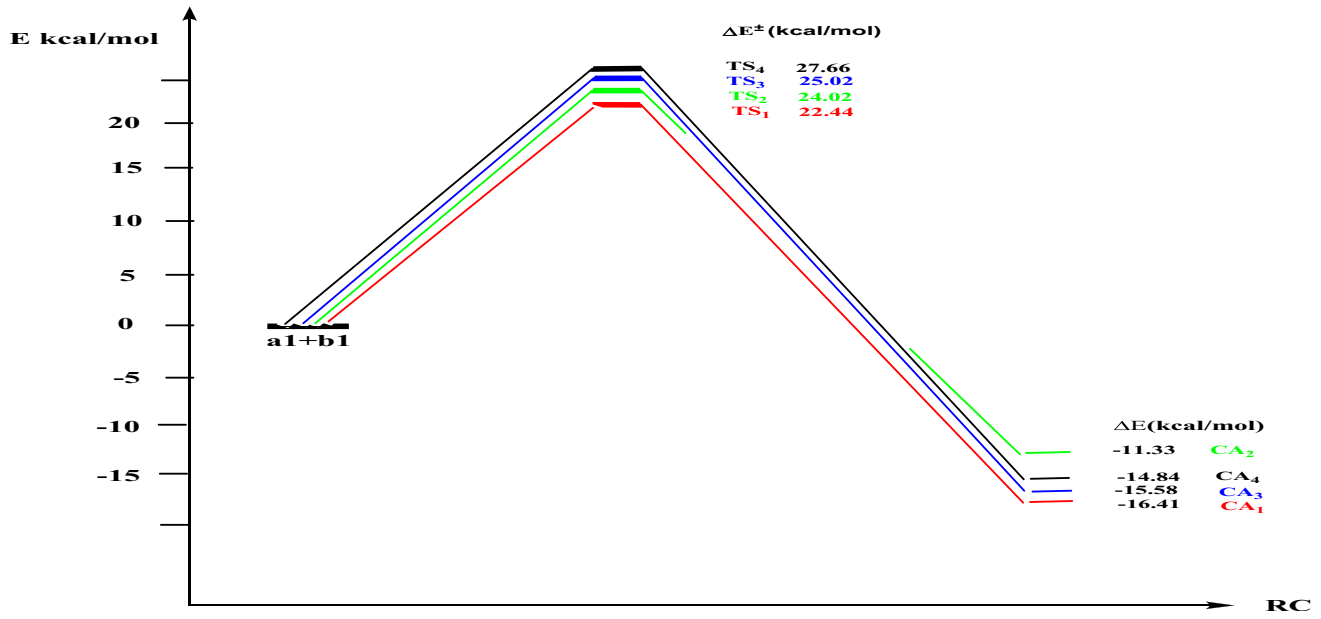

Scheme 3 Energy profiles for the competitive reactive pathways associated with the 32CA reaction between nitrone a1 and alkene b1

energy of this reactive channel to 42.66 kcal mol^{-1}, as a consequence of the unfavorable negative activation entropy, $\Delta S = -52.27$ kcal mol^{-1} K^{-1}. Moreover, this 32CA reaction shows a slightly endothermic character, which accounts for its reversibility, whereas CA_1 is favored thermodynamically because it is the more stable cycloadduct. Consequently, it is expected to obtain a single isomer (CA_1) from this 32CA reaction, as observed experimentally.

When examining the reaction between nitrone **a1** and alkene **b1**, the lengths of the newly formed bonds, C1-C3 and C2-O, for TS_1 (TS_3) are 2.04(2.00) and 2.15(2.17) Å, respectively. Conversely, the lengths of the formed bonds, C2-C3 and C1-O, for TS_2 (TS_4) are 2.08(2.08) and 2.03(1.95) Å, respectively. Analysis of the geometries at the TS structures given in Fig. 2 shows that the asynchronous bond formation processes for TS_1, TS_3, and TS_4 are greater compared to that of TS_2.

The concept of bond order (BO) [26] provides a valuable tool for conducting a thorough analysis of the degree of bond formation or breakage throughout a reaction pathway. This theoretical approach has proven effective in studying the molecular mechanism of chemical reactions. The evaluated bond order of formed bonds C1-C3 and C2-O at transition states are 0.476 and 0.340 for TS_1 and 0.507 and 0.3337 for TS_3. The evaluated bond order of O-C1 and C2-C3 bonds that form bonds at transition states are 0.463 and 0.405 for TS_2 and 0.49 and 0.452 for TS_4, respectively. Therefore, the asynchronous process of C1-C3 bond formation is more advanced than the O-C2 bond for the TS_1 and TS_3, while the asynchronous process of O-C1 bond formation is more advanced than the C2-C3 bond for the TS_2 and TS_4. These results show that this reaction follows an asynchronous concerted mechanism.

The polarity of the 32CA reaction has been examined by calculating the global electron density transfer (GEDT) at the transition states (TSs) using natural population analysis (NPA) [18]. The natural atomic charges at

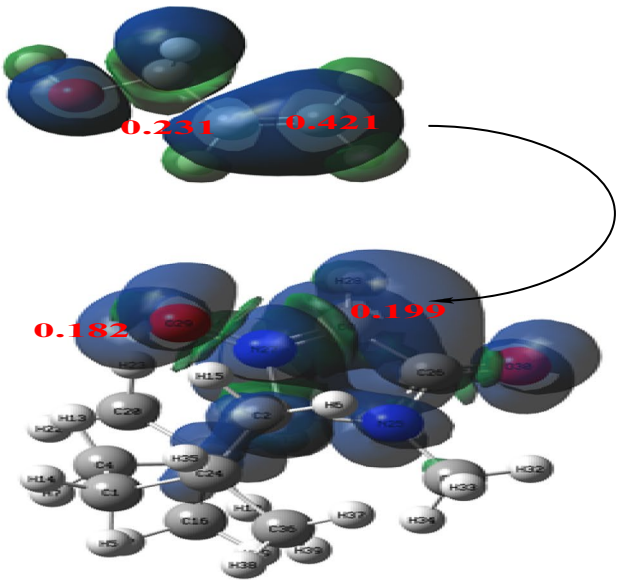

Fig. 2 3D maps of ASD for radical cation of alkene b1 with the nucleophilic P_k^- Parr functions and the radical anion of nitrone a1 with electrophilic P_k^+ Parr functions

the TSs were determined based on the residual charge at alkene b1. The positive sign of the GEDT signifies that the flux of GEDT occurs from alkene **b1** towards nitrone **a1**. Consequently, alkene b1 is identified as a nucleophile, while nitrone a1 acts as an electrophile. The values of GEDT are 0.083e at TS_1, 0.075e at TS_2, 0.077e at TS_3, and 0.083e at TS_4. These low values indicating the non-polar nature of this 32CA reaction.

(b) Analysis based on CDFT reactivity indices

Research focused on polar organic reactions has demonstrated the importance of studying reactivity indices using conceptual density functional theory (CDFT) [27]. This study points to the useful contribution these indices can make to understanding reactivity, particularly in polar cycloadditions. Global DFT indices, including electronic chemical potential (μ), chemical hardness (η), electrophilicity (ω), and nucleophilicity (N), were examined in the ground state of the reactants involved in this 32CA reaction. The corresponding values of these indices are shown in Table 2.

The electronic chemical potential of nitrone **1a**, $\mu = -4.29$ eV, is lowest than that of alkene **b1**, $\mu = -3.43$eV, indicating that along reactions the global electron density transfer (GEDT) will flux from the alkene **b1** to nitrone **a1**, in great agreement with the GEDT calculated at the TSs. The electrophilicity and nucleophilicity values for nitrone 1a, with ω at 1.88 eV and N at 2.38 eV, classify it as a moderate electrophile and a moderate nucleophile according to the electrophilicity [28] and nucleophilicity [29] scales. Similarly, alkene b1, with ω at 0.88 eV and N at 2.17 eV, is classified as a marginal electrophile and a moderate nucleophile. As a consequence, based on electrophilicity, alkane **b1** rests as a nucleophile. However, according to nucleophilicity, nitrone 1a is identified as a nucleophile, which contradicts the previous results.

To predict regioselectivity in cycloaddition reactions, recent research proposes that the most favorable reactive pathway involves the initial two-center interaction between the more electrophilic and nucleophilic centers of the two reactants. Geerlings et al. [27] have proposed electrophilic Pk^+ and nucleophilic Pk^- Parr functions, derived from spin electron density changes via the GEDT process, as an important tool for the study of local reactivity. As a consequence, an analysis of nucleophilic Pk-Parr functions for alkene **b1** and electrophilic Pk^+ Parr functions for nitrone **a1** is performed to predict the most favorable two-center electrophile/nucleophile interaction in this 32CA reaction. This analysis aims to elucidate the regioselectivity observed experimentally.

Figure 2 displays three-dimensional (3D) representations of the atomic spin density (ASD) maps for the two systems: the radical cation of alkene **b1** and the radical anion of nitrone **a1**. Figure 2 also contains the values of the nucleophilic Parr functions for alkene **b1** and the electrophilic Parr functions for nitrone **a1**. From Fig. 2, we can see that in this 32CA reaction, analysis of the electrophilic Parr functions of the nitrone shows that carbon atom C3 (see Scheme 2 for atom numbering) is the most electrophilic of these molecules, $P = 0.199$. On the other hand, the nucleophilic Parr functions of alkene b1 are mainly concentrated on carbon atom C1 ($P = 0.421$), leading to the formation of regioisomer CA_1, in good agreement with experimental results.

Topological analyses

(a) Electrostatic potential (ESP) analysis

ESP is a potent topological colored map with a variety of active electronic sites in the structural system. The results of this analysis were summarized in Fig. 3 for TS_1 of the studied reaction. As the electrostatic potential assigned high electronic density in the blue surface regions, this refers to less tightly located electrons. Additionally, the electronic density was postulated as high to form as rich electronic regions, so these sites can react with electrophiles (nucleophilic attack of O1 on C2). This fact may be attributed to a significant electron withdrawal effect of methylol (CH_2OH) substituent, leaving a partial positive charge on the C2 reactive site. Based on the ESP map, the most nucleophilic active sites represented in oxygen attached to nitrogen in the five-membered ring reactant (a1). The red regions represent the poor-electronic sites that appeared in other regions over the system.

(b) Reduced density gradient/non-covalent interaction (RDG-NCI) analysis

Some important non covalent interactions were generated by the aid of RDG technique accompanied with specified color codes [24]. Figure 4 shows RDG dramatic color change over the system according to sign

Table 2 Frontier orbitals energies (HOMO /LUMO) and global properties of nitrone (**a1**) and alkene (**b1**) (values are calculated by eV)

	E_{HOMO}	E_{LUMO}	μ	η	ω	N
a1	−6.73	−1.84	−4.29	4.88	1.88	2.38
b1	−6.95	0.084	−3.43	3.43	0.84	2.17

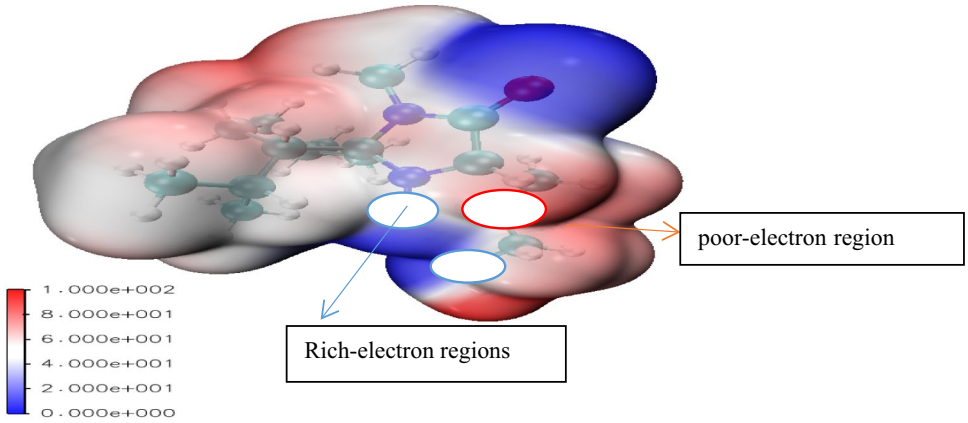

Fig. 3 ESP map for TS_1 with colored potential scale

(λ_2) ρ index, where the green spikes describe VdW electrostatic interaction and red spike refers to strong repulsion interactions. H-bond formation is a current state support the stability of generated transition state. Some H-bond character appeared at in the interaction centers. The presence of a significant repulsion interaction in the reactive region indicating delocalization of electronic density emerged from the two reactive parts. This fact mainly is due to other substituents like non-interactive O of (**a1**) and CH_2OH of b1 visualized in Fig. 4a. The spikes appeared in Fig. 4b based on the type of interaction present in the system is mentioned above.

(c) Electron localization function

Another supported analysis describing the main path of reaction mechanism is ELF. This type can predict the electron localized areas on the system surface and then specify the nature of the bond between atoms. Figure 5 displays two planes (N-C3-C1 and N–O-C2) of 2D surface map for the formed TS_1. As the plane is generated with specifying three successive atoms, the map shows a significant variation in electron localization density with a characteristic color code [25] around the studied 3 atoms plane. In Fig. 5a, the electronic density around the interactive centers, C3 and C1, is nearly negligible as the electronic red color parts distributed away from the main centers. While in Fig. 5b, the electronic density less deformed and significantly localized O and directed to C2. This discussion confirmed the initial nucleophilic attack step of the partially negative O on the partially positive C2.

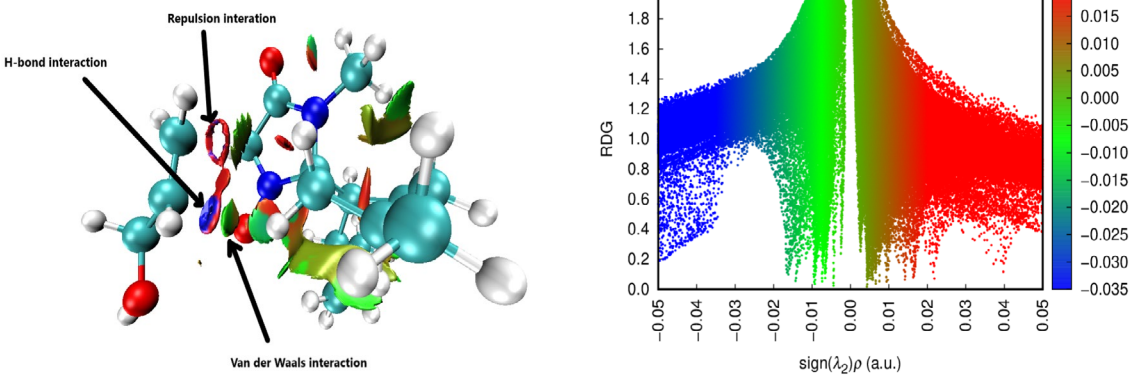

Fig. 4 RDG-NCI map of the studied system, **a** colored interactive map structure, **b** RDG spikes-plot, with known interactions color codes

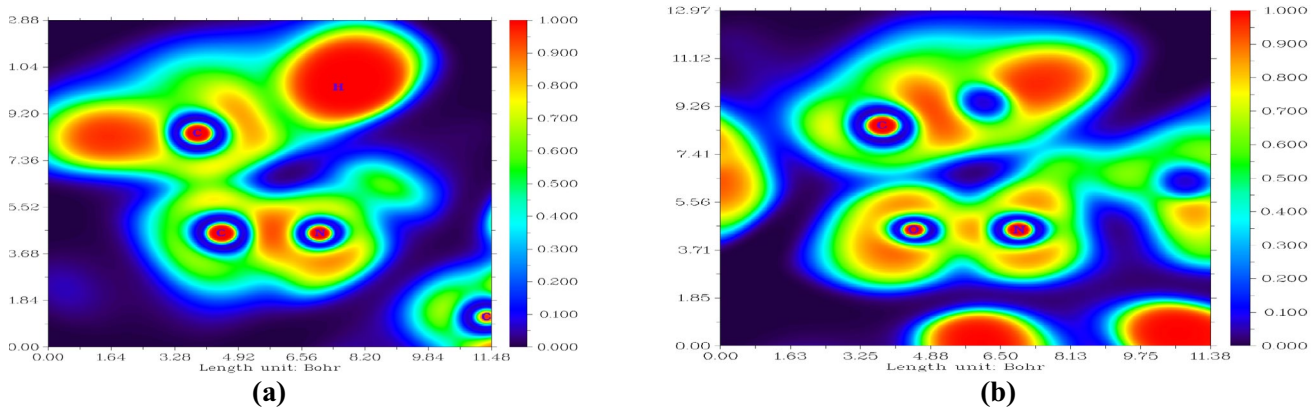

Fig. 5 ELF map of 3-atoms plane for TS_1, **a** N-C3-C1 plane and **b** N–O-C2 plane

Conclusions

In this work, we have investigated theoretically the regio- and stereoselectivities of the [3 + 2] cycloaddition (32CA) reaction of nitrone **a1** with the substituted alkene **b1**. For the theoretical investigation, we have performed a computational study of the mechanism and the regio- and stereoselectivities of this reaction using DFT methods at the B3LYP/6-31G(d,p) theoretical level. The principal conclusions that can be deduced from our results are as follows:

(i) Our results demonstrate that the 32CA reaction between nitrone a1 and the substituted alkene b1 exhibit high regioselectivity and stereoselectivity (specifically, pathway 1.3). This selectivity leads kinetically and thermodynamically to the formation of a single cycloadduct CA_1, which is in excellent agreement with experimental observations.

(ii) The examination of global electron density transfer (GEDT) and bond order of transition states (TSs) reveals that the 32CA reaction occurs through a non-polar asynchronous mechanism between nitrone 1a and alkene b1. This is due to the nucleophilic nature of both reagents.

(iii) Analysis of the DFT reactivity indices at the ground state of the reagents involved in this 32CA reaction indicates that alkene b1 is a nucleophile and nitrone a1 is an electrophile in complete agreement with the calculated global electron density transfer (GEDT) analysis at TSs.

(iv) The analysis of local reactivity indices based on Parr functions method predicts correctly the regioselectivity observed experimentally.

(v) ESP, RDG-NCI, and ELF analyses were used to determine the active sites; distinguish hydrogen bonds, van der Waals interactions, and steric repulsive interactions; and predict the electron localized areas in the reacting system.

Author contribution The author wrote the main manuscript text.

Funding This work was supported by the Ministry of Higher Education and Scientific Research of the Algerian Government [project PRFU Code: B00L01UN280120230003].

Declarations

Competing interests The authors declare no competing interests.

References

1. Tufariello JJ (1984) In 1, 3-dipolar cycloaddition chemistry, ed. A Padwa, John Wiley & Sons, New York (b) Torssell KBG (1988) In nitrile oxides, nitrones and nitronates in organic synthesis. VCH, New York (c) Jones R CF, Martin JN (2002) The chemistry of heterocyclic compounds. In synthetic applications of 1, 3- dipolar cycloaddition chemistry toward heterocycles and natural products. John Wiley & Sons, New York
2. Frederickson M (1997) Tetrahedron 53: 403–425 (b) Gothelf K V, Jorgensen K A (1998) Chem. Rev 98:863–909
3. Seerden JPG, Boeren MMM, Scheeren HW (1997) Tetrahedron 53:11843
4. Patterson W, Cheung PS, Ernest MJ (1992) J Med Chem 35:507. Wagner E, Becan L, Nowakowska E (2004) Bioorg Med Chem 12:265
5. Volkan Y, Disli A, Serkan Y, Hatice O, Gulay D (2019) GU J Sci 32(1):78–89
6. Bhaskar C, Esmita C (2018) I J Chem 57:1501–1508
7. Nacereddine AK, Yahia W, Bouacha S, Djerourou A (2010) Tetrahedron Lett 51:2617–2621
8. Mousa S, Zeinab KC (2019) JMGM 92:256–266
9. Ewar D, Agnieszka KZ, Magdalena K, Radomir J (2018) JMM 24:329
10. Kang KH, Pae AN, Choi KI, Cho YS, Chung BY, Lee JE, Jung SH, Koh HY, Lee HY (2001) Tetrahedron Lett 42:1057–1060
11. Chen S, Ren J, Wang Z (2009) Tetrahedron 65:9146–9151
12. Habib M, Hassiba C, Asma M, Mejdi S, Kaïss A, Rui MVA, Ali B, Lotfi A, Boulbaba S (2019) Appl Biochem Biotechnol 187:1113–1130
13. Frisch MJ, Trucks GW, Schlegel HB, Scuseria GE, Robb MA, Cheeseman JR, Scalmani G, Barone V, Mennucci B, Petersson GA, Nakatsuji H, Caricato M, Li X, Hratchian HP, Izmaylov AF,

Bloino J, Zheng G, Sonnenberg JL, Hada M, Ehara M, Toyota K, Fukuda R, Hasegawa J, Ishida M, Nakajima T, Honda Y, Kitao O, Nakai H, Vreven T, Montgomery JA, Peralta Jr JE, Ogliaro F, Bearpark M, Heyd JJ, Brothers E, Kudin KN, Staroverov VN, Kobayashi R, Normand J, Raghavachari K, Rendell A, Burant JC, Iyengar SS, Tomasi J, Cossi M, Rega N, Millam JM, Klene M, Knox JE, Cross JB, Bakken V, Adamo C, Jaramillo J, Gomperts R, Stratmann RE, Yazyev O, Austin AJ, Cammi R, Pomelli C, Ochterski JW, Martin RL, Morokuma K, Zakrzewski VG, Voth GA, Salvador P, Dannenberg JJ, Dapprich S, Daniels AD, Farkas O, Foresman JB, Ortiz JV, Cioslowski J, Fox DJ (2009) Gaussian 09, revision A.02, Gaussian Inc, Wallingford CT

14. Schlegel HB (1982) J Comput Chem 3:214–218
15. Gordon MH, Pople JA (1988) J Chem Phys 89:5777–5786
16. Gonzalez C, Schlegel HB (1990) J Phys Chem 94:5523–5527
17. Gonzalez C, Schlegel HB (1991) J Chem Phys 95:5853–5860
18. Reed AE, Weinstock RB, Weinhold F (1985) J Chem Phys 83:735–746 (b) Reed AE, Curtiss LA, Weinhold F (1988) Chem Rev 88:899–926
19. Simkin BY, Sheikhet I (1995) Quantum chemical and statistical theory of solutions: a computational approach. Ellis Horwood, London
20. Hehre WJ, Radom L, Schleyer P, Pople JA (1986) Ab initio Molecular Orbital Theory. Wiley, New York
21. Domingo LR, Ríos-Gutiérrez M, Patricia P (2016) Molecules 21:748
22. Kohn W, Sham LJ (1965) Phys Rev 140:1133
23. Domingo LR, Pérez P (2014) Org Biomol Chem 11:4350
24. Lu T, Chen F (2012) Multiwfn: a multifunctional wave function analyzer 5:33
25. Humphrey W, Dalke A, Schulten K (1996) J Molec. Graphics 14:33–38
26. Wiberg KB (1968) Tetrahedron 24:1083
27. Domingo LR, Rios-Gutierrez M, Perez P (2016) Molecules 21:748
28. Domingo LR, Aurell MJ, P´erez P, Contreras R (2002) Tetrahedron 58:4417
29. Jaramillo P, Domingo LR, Chamorro E , P´erez P (2008) J Mol Struct 68:865